

USER OPERATION OF SUB-PICOSECOND THz COHERENT TRANSITION RADIATION PARASITIC TO A VUV FEL

S. Di Mitri^{†,1}, N. Adhlakha, E. Allaria, L. Badano, G. De Ninno², P. Di Pietro, G. Gaio, L. Giannessi³, G. Penco, A. Perucchi, P. Rebernik Ribic, S. Spampinati, C. Spezzani, M. Trovo', M. Veronese, Elettra - Sincrotrone Trieste S.C.p.A., Basovizza, Trieste, Italy

S. Lupi, Sapienza University of Rome, Italy

E. Roussel, PhLAM/CERCLA, Villeneuve d'Ascq Cedex, France

Federica Piccirilli, IOM-CNR, Trieste, Italy

²also at University of Nova Gorica, Slovenia

³also at ENEA C.R. Frascati, Rome, Italy

Abstract

Coherent transition radiation is enhanced in intensity and extended in frequency spectral range by the electron beam manipulation in the beam dump beam line of the FERMI FEL, by exploiting the interplay of coherent synchrotron radiation instability and electron beam optics [1]. Experimental observations at the TeraFERMI beamline [2] confirm intensity peaks at around 1 THz and extending up to 8.5 THz, for up to 80 μ J pulse energy integrated over the full bandwidth. By virtue of its implementation in an FEL beam dump line, this work might stimulate the development of user-oriented multi-THz beamlines parasitic and self-synchronized to VUV and X-ray FELs.

INTRODUCTION

This study demonstrates that coherent transition radiation (CTR) with sub-picosecond duration, up to nearly 80- μ J pulse energy in the THz gap, was produced by exploiting the electrons' interaction with coherent synchrotron radiation (CSR) emitted in the post-undulator dispersive region of the VUV FERMI free electron laser (FEL) [3,4]. THz radiation with those characteristics finds application in experiments involving, for example, resonantly exciting collective modes as phonons, polarons, charge/spin-density-wave gaps, superconducting gaps in high-temperature superconductors and plasmons.

A sketch of the FERMI electron beam delivery system is shown in Fig. 1. Only the first magnetic bunch length compressor (BC1) is routinely active for lasing. Start-to-end simulations of the electron beam dynamics were carried out, for diverse linac settings, from the Gun (G) through the linac sections (L0-L4) until the Main Beam Dump (MBD), where the Al target for CTR emission is installed. The bottom plot is a 3-D rendering of the MBD, from the FEL post-undulator region to the dump. The active dipole magnets, named "Dipole 1" and "Dipole 2" in the figure, are long 1.12 m and 2.44 m, with bending angles of 15.7 deg and 31.4 deg respectively. Three quadrupoles between "Dipole 1" and "Dipole 2" tune the momentum compaction (R_{56}) of the beam line. CTR is emitted at the 1 μ m-thick Al target. Four quadrupoles installed upstream of the first dipole control the beam envelope along the line without affecting the R_{56} value. The transverse RMS beam sizes at

the CTR target are kept smaller than 0.5 mm. Steering magnets and beam position monitors (not shown) allow control of beam trajectory. While electrons are bent and eventually dumped, FEL propagates straight to the downstream experimental hall (EH).

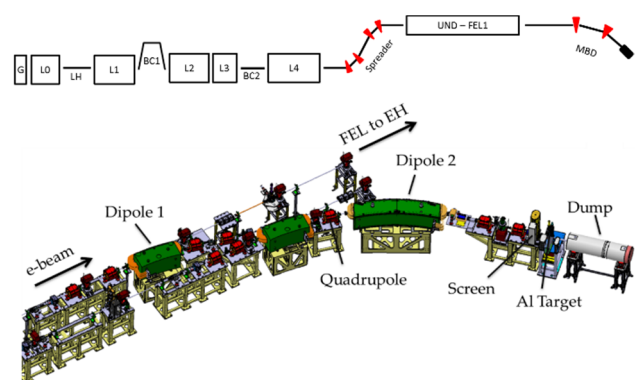


Figure 1: Sketch (not to scale) of the FERMI electron beam delivery system (top) and MBD line. Published in [1].

CSR-DRIVEN BUNCH COMPRESSION

The full width duration of the electron bunch prepared for lasing, thus entering the MBD line, is approximately 1 picosecond full width. In order to maximize transition radiation intensity at frequencies of 1 THz and above, a sub-picosecond charge density structure, *i.e.*, a kA-level current spike has to be generated in the bunch passing through the MBD, before reaching the Al target. Doing so, radiation can be emitted coherently in the multi-THz range at several tens of μ J-energy per pulse.

The FERMI dump line was designed to enhance the CSR wakefield by adopting relatively long and large angle dipole magnets, and for producing a tuneable but yet relatively large and positive R_{56} . This term couples with the CSR-induced negative energy chirp [5,6] and, as shown in the following, generates a \sim 100 fs-long leading current spike that radiates coherently in the THz range. The CSR-induced single particle energy deviation is actually correlated with z and, in particular, a negative linear chirp $h_1 < 0$ is produced at the bunch head, *i.e.*, leading particles are moved to higher energy with respect to trailing ones.

At the linac exit, the linear energy chirp in the head of the bunch was approximately -2 MeV/ps (see Fig.2). The

Content from this work may be used under the terms of the CC BY 3.0 licence (© 2019). Any distribution of this work must maintain attribution to the author(s), title of the work, publisher, and DOI

energy chirp induced by the CSR wakefield in the two dipole magnets shown in Fig.1, and according to beam parameters reported in Tab.1, is predicted to be -6 MeV/ps or $h_{1,CSR} \approx -23$ m⁻¹, and therefore it dominates the time-compression of the bunch head through the dump line. An optics setting which provides $R_{56} = 20$ mm, for instance, is expected to increase the bunch head peak current by a factor ~ 2 , thus reaching the kA-level at the target.

Table 1: Electron Beam Parameters of the THz Experimental Sessions; (*) Means “at the Linac End”

Parameter	Value	Units
Bunch Charge	0.7	nC
Initial Duration	2.8	ps
Mean Energy*	1308 / 871	MeV
Hor. Emittance*	2.1 / 1.8	μm
Vert. Emittance*	1.7 / 1.5	μm
Compr. Factor*	8 / 8, 11	
Bunch Duration*	0.35 / 0.35, 0.25	ps
Peak Current*	560 / 560, 750	A
R_{56} of the Dump Line	5, 19 / 37	mm

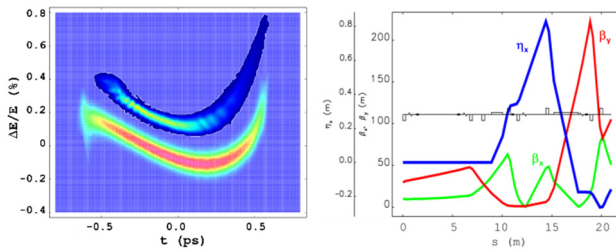


Figure 2: Left: simulated and measured electron beam longitudinal phase space at the end of the FERMI linac, at the beam energy of 1308 MeV; bunch head is at negative time coordinates. The current profile is approximately flat at the level of ~ 600 A (the measured phase space is upper-shifted w.r.t. the simulation for visualization). Right: betatron functions ($\beta_{x,y}$) and horizontal energy-dispersion function (η_x) from the exit of the FERMI undulator to the Al target, calculated starting from Twiss parameters measured in front of the undulator, and for the actual quadrupoles setting. ($R_{56} = 19$ mm). Published in [1].

CHARACTERIZATION OF CTR

Table 1 summarizes the electron beam parameters and the accelerator setting discussed so far. Two additional linac configurations at lower beam energy are also shown, and discussed below. For each configuration, the aforementioned control of longitudinal phase space and optics was accomplished.

CTR pulse energy and spectrum were calculated by applying the generalized Ginzburg-Frank formula, corrected by the prescription for far-field emission [7], to the electron bunch distribution simulated at the Al target. The expected value of the photon pulse energy was compared with the one measured by means of a pyroelectric detector installed after a Diamond window, in proximity of the target.

In order to demonstrate that, as predicted by the model, a larger R_{56} increases the bunch head peak current and

therefore the THz radiation intensity, pulse energies were measured for two optics settings of the dump line, named “OS1” ($R_{56}=5$ mm) and “OS2” ($R_{56}=19$ mm), at fixed CF in the linac (beam and linac parameters in Tab. 1, $E=1308$ MeV). Figure 3a shows the electron beam current profiles corresponding to OS1 and OS2, simulated at the target starting from the measurement shown in Fig.2-left plot, plus an unphysical case *without* CSR. A 3 kA, 100 fs-long current spike is obtained for OS2. In this case, the CTR calculation in Fig. 3b reveals that a significant frequency content is present up to 8.5 THz. Namely, at 8.5 THz the emission still contains 0.5 μJ energy over a 10% bandwidth, a value which is plausibly high enough to induce nonlinear effects in matter. The theoretical pulse energies integrated over the bandwidth 0.01–10 THz and represented by solid lines in Fig. 3c, are compared with the measured ones (dots with error bar). A striking agreement is achieved only when CSR is included in the simulations. It is worth mentioning that the multi-THz frequency content predicted in Figs. 3b and 4b reflects typical spectral measurements [8] collected during TeraFERMI operation, as shown in Fig.5.

To additional highlight the relevance of the CSR wakefield for the production of THz radiation, another series of measurements was carried out with a fixed R_{56} in the dump line (beam and linac parameters in Tab. 1, $E=871$ MeV), and for two values of the linac CF, named “CF1” (CF=8) and “CF2” (CF=11). A shorter bunch at the entrance of the dump line is expected to emit stronger CSR field. This produces a larger negative chirp and therefore a higher leading current spike, thus more intense THz emission. Figure 4a shows two current profiles simulated at the Al target for the two values of the linac CF, plus an unphysical case *without* CSR. Similarly to Fig. 3c, the measured pulse energies in Fig.4c confirm the expectations only when CSR is included in the simulations.

A summary of the experimental settings of the dump line, of the simulated and of the measured THz-pulse energy is given in Table 2. The uncertainty on the pulse energy value is dominated by the RMS fluctuation of the THz signal collected by the detector, which is typically smaller than 10%. The striking agreement of measured and predicted pulse energies for all the cases considered, and the energy reduction found in the simulation when CSR is not included, are a conclusive demonstration of the validity of our modelling.

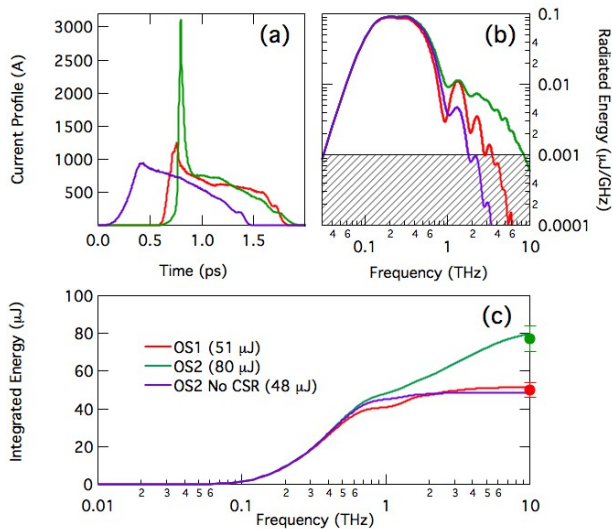


Figure 3: Simulated electron bunch current profiles at the Al target for two optics settings of the dump line (OS1-red and OS2-green). For comparison, a case without CSR in the dump line dipole magnets is shown (violet), see also Tab.2. (b) Calculated CTR spectra. A threshold of 20 dB from the main intensity peak is indicated by the gray area. (c) Solid lines: CTR pulse energy integrated over the frequency range 0.01–10 THz and calculated from the above current profiles. Dots with error bars: measured pulse energy, see also Tab.2. Published in [1].

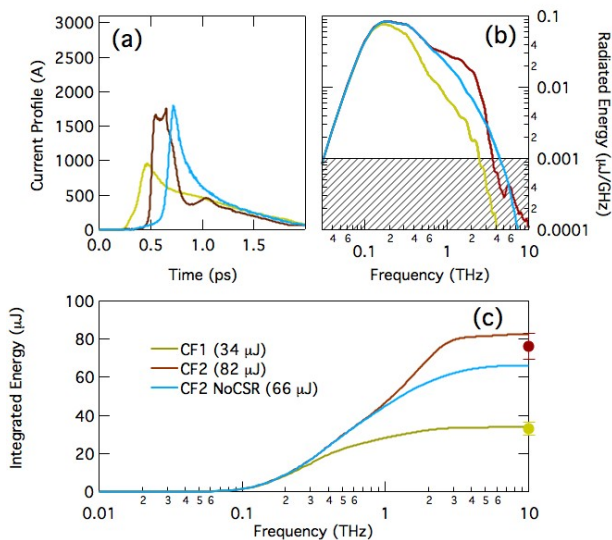


Figure 4: (a) Simulated electron bunch current profiles at the Al target for two compression factors in the linac (CF1-yellow and CF2-brown) and fixed R_{56} in the dump line. For comparison, a case without CSR in the dump line dipole magnets is shown (cyan), see also Tab.2. (b) Calculated CTR spectra. A threshold of 20 dB from the main intensity peak is indicated by the gray area. (c) Solid lines: CTR pulse energy integrated over the frequency range 0.01–10 THz and calculated from the above current profiles. Dots with error bars: measured pulse energy, see also Tab.2. Published in [1].

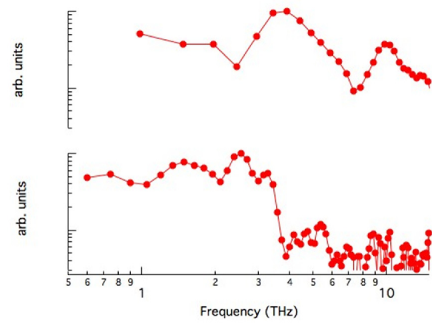


Figure 5: Two examples of experimental FTIR spectra acquired with different machine settings at the TeraFERMI laboratory. Published in [8].

Table 2: Momentum Compaction of the Beam Dump Line (R_{56} , Bunch Duration at Its Entrance ($\sigma_{t,i}$, Measured and Simu-Lated Pulse Energies in the 0.01–10 THz Range

Configura- tion	R_{56} [mm]	$\sigma_{t,i}$ [ps]	E [μJ] simul.	E [μJ] meas.
OS1	5	0.35	51	50 ± 4
OS2	19	0.35	80	77 ± 7
OS2 No CSR	19	0.35	48	
CF1	37	0.35	34	33 ± 3
CF2	37	0.25	82	76 ± 7
CF2 No CSR	37	0.25	66	

CONCLUSIONS

The enhancement of the CTR pulse energy as a function of the momentum compaction of the FERMI dump line and of the incoming bunch length was verified experimentally. The systematic agreement of measured and calculated pulse energy for different accelerator and dump line optics settings confirms the fundamental role played by the CSR wakefield in generating a ~ 0.1 ps long, \sim kA level-current spike in the bunch head, when a positive linear momentum compaction is established. Since the electron beam manipulation for CTR emission occurs after lasing, the scheme allows the TeraFERMI photon beamline to run in parasitic mode to the FEL. The THz pulse is self-synchronized to the FEL emission thus opening, in principle, a wide range of scientific applications in pump-probe configurations. By virtue of the relatively simple set up, the scheme promises dissemination of user-oriented multi-THz beamlines at existing and planned FEL infrastructures.

REFERENCES

- [1] S. Di Mitri et al., “Coherent THz Emission Enhanced by Coherent Synchrotron Radiation Wakefield”, *Scientific Reports*, vol. 8, p. 11661, 2018. doi:10.1038/s41598-018-30125-1
- [2] A. Perucchi et al., “TeraFERMI: a superradiant beamline for THz nonlinear studies at the FERMI free electron laser facility”, *Synch. Rad. News* 4, vol. 30, 2017. doi:10.1080/08940886.2017.1338423

Content from this work may be used under the terms of the CC BY 3.0 licence (© 2019). Any distribution of this work must maintain attribution to the author(s), title of the work, publisher, and DOI

- [3] E. Allaria et al., “Highly coherent and stable pulses from the FERMI seeded free-electron laser in the extreme ultraviolet”, *Nat. Photon.*, vol. 6, p. 699, 2012. doi:10.1038/nphoton.2012.233
- [4] E. Allaria et al., “Two-stage seeded soft-X-ray free-electron laser”, *Nat. Photon.*, vol. 7, p. 913, 2013. doi:10.1038/nphoton.2013.277
- [5] E. L. Saldin, E. A. Schneidmiller, and M. V. Yurkov, “On the coherent radiation of an electron bunch moving in an arc of a circle”, *Nucl. Instrum. Meth. Phys. Research, Sect. A* vol. 398, p. 373, 1997. doi:10.1016/S0168-9002(97)00822-X
- [6] R. A. Bosch, “Reduction of energy chirp by the wake of coherent synchrotron radiation”, *Phys. Rev. Special Topics – Accel. Beams*, vol. 13, p. 110702, 2010. doi:10.1103/PhysRevSTAB.13.110702
- [7] S. Casalbuoni, B. Schmidt, and P. Schmüser, “Far-Infrared Transition and Diffraction Radiation”, TESLA Report 2005-15 (2005).
- [8] P. Di Pietro, N. Adhlakha, F. Piccirilli, L. Capasso, C. Svetina, S. Di Mitri, M. Veronese, F. Giorgianni, S. Lupi and A. Perucchi, “TeraFERMI: A Superradiant Beamline for THz Nonlinear Studies at the FERMI Free Electron Laser Facility”, *Synchr. Rad. News*, vol. 30, Issue 4, p. 36, 2017. doi:10.1080/08940886.2017.1338423